Quantitative Optical Coherence Tomography Imaging of Cell Death

Golnaz Farhat[1,3,4], Victor X.D. Yang[3,5,6], Michael C. Kolios[1,6] and Gregory J. Czarnota[1,2,3,4]
[1]Departments of Medical Biophysics and [2]Radiation Oncology, Faculty of Medicine, University of Toronto, Toronto, ON, Canada
[3]Imaging Research and [4]Department of Radiation Oncology, Sunnybrook Health Sciences Centre, Toronto, ON, Canada
[5]Ontario Cancer Institute, University Health Network, Toronto, ON, Canada
[6]Department of Physics, Ryerson University, Toronto, ON, Canada.
golnaz.farhat@utoronto.ca

Abstract: A quantitative technique measuring OCT backscatter power is used to detect three modes of cell death in acute myeloid leukemia cells. Changes in backscatter are correlated with structural differences observed in histological staining of cells.

OCIS codes: (110.4500) Optical coherence tomography; (170.3880) Medical and biological imaging.

1. Introduction

The response to a cancer treatment is typically evaluated by measuring changes in tumor size which occur several weeks after the start of therapy. However, structural changes resulting from cell death in responding cells occur as early as 24 hours after the administration of chemotherapy or radiation. Monitoring early response to treatment could prevent the continuation of ineffective treatments, reducing unnecessary side effects and potentially improving treatment outcomes.

During cancer cell death, characteristic structural transformations occur at the cellular level changing the mechanical and optical properties of cells. Recently, variations in the optical attenuation coefficient of human fibroblast cell samples have been detected as a result of cell death *in vitro* [1]. Changes in relative tissue scattering have also been detected between viable and non-viable tumor regions in a mouse tumor model using optical frequency domain imaging [2]. We have previously used quantitative spectroscopic methods with high frequency ultrasound (HFUS) imaging to detect cell death both *in vitro* and *in vivo* [3, 4]. Optical coherence tomography (OCT) and HFUS share many similarities in manners of data acquisition and image formation, but differ in their contrast mechanisms. Based on the similarities, we have applied techniques used previously for cell death monitoring with HFUS to OCT.

Here we test the hypothesis that structural changes occurring within dying cells will induce observable changes in measured OCT backscatter signals. For this study, three types of cell death were induced in acute myeloid leukemia (AML) cells: apoptosis, mitotic arrest and necrosis. Morphologically, apoptosis is characterized by nuclear condensation and fragmentation, followed by blebbing of the cell membrane and disintegration of the cell into apoptotic bodies. It has been demonstrated that changes in mitochondrial morphology may also be associated with apoptosis [5]. Cells arrested in mitosis are slightly enlarged and show increased chromatin content due to the condensation and doubling of chromosomes in preparation for cell division. Necrosis is characterized by initial cellular and organelle swelling (oncosis) followed by nuclear shrinkage, budding of the cell membrane and cell lysis [6, 7].

2. Materials and methods

Cell samples were prepared with acute myeloid leukemia cells (AML-5). Approximately $1X10^9$ AML cells obtained from frozen stock samples were grown at 37°C in suspension flasks containing 150mL of α-minimal medium supplemented with 1% streptomycin and 5% fetal bovine serum.

Apoptosis was induced by treating the cells with the chemotherapeutic agent *cis*-platinum, a DNA intercalater which causes a p53 dependant apoptosis [8]. Cells were treated in suspension at 10 µg/mL for 24 hours [9]. Mitotic arrest was induced using the chemotherapeutic agent colchicine. This drug inhibits the formation of tubulin, causing the arrest of cells at metaphase in the mitosis cycle [10]. Colchicine was administered in suspension at 0.1µg/mL 24 hours prior to cells being processed for imaging [3]. Cells were washed with phosphate buffered saline (PBS) and pelleted in a benchtop swing bucket centrifuge in a flat bottom ependorff tube producing a densely packed cell sample approximately 1 cm in diameter and 0.5 cm in height. An additional sample was produced from untreated cells to serve as a control. Necrotic cell death was measured in a separate experiment. Two untreated cell samples were used: the first served as a control sample while the second was immersed in PBS and maintained at room temperature for 24 hours to induce necrosis. The absence of growth medium during this period results in a lack of ATP produced by the cells which, in turn, induces ionic pump failure in the cell membrane, leading to oncosis and

eventually necrosis [7]. Immediately after the completion of OCT imaging, cell samples were fixed in 10% formalin for 48 hours and subsequently paraffin embedded and processed for haematoxylin and eosin (H&E) staining.

Optical coherence tomography images and data were acquired using a Thorlabs Inc. (Newton, NJ) swept source OCT (OCM1300SS) system. Data were collected in the form of 14-bit OCT interference fringe signals. For each sample, 2 dimensional (2D) data sets containing 512 axial scans were collected in 10 planes spaced at least 10µm apart. Each 2D scan covered a total transverse distance of 3 mm and a depth of 3 mm.

From each 2D scan a region of interest (ROI) covering a depth of 250µm and a lateral distance of 600 µm was selected. These distances correspond to 190 and 460 times the central wavelength, respectively. Normalized backscatter power spectra were obtained by calculating the Fourier transform of the complex interference signals corresponding to the selected ROIs and normalizing the squared magnitude of these spectra by the power spectrum computed from a titanium dioxide reference phantom. The resulting normalized power spectra were integrated over the -6 dB bandwidth of the light source to calculate the integrated backscatter (IB). An average IB value was calculated for each 2D ROI. Error bars were obtained for each sample by calculating the standard deviation of the IB over the 10 ROIs acquired.

3. Results

B-Mode OCT images in Fig. 1 demonstrated changes in intensity between the control sample and treated samples for both experiments. Backscatter power spectra (Fig. 2) for all three experiments also indicated increases in backscatter intensity observed for the cisplatin and colchicine treated cells (approximately 10% and 100% respectively) and a decrease (50%) for the cells decaying in PBS. Integrated backscatter is related to backscatter intensity and the tables in Fig. 2 also indicate similarly significant changes.

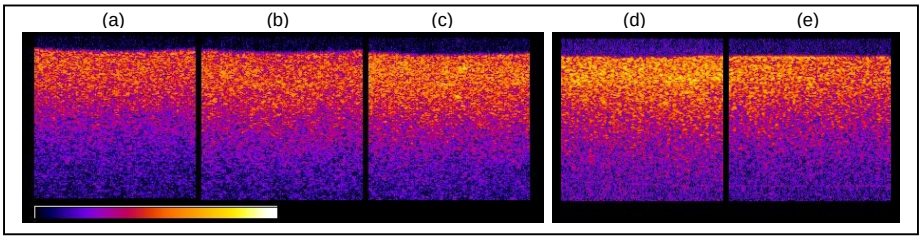

Fig. 1. Optical coherence tomography B-mode images of centrifuged cell samples. Left panel: (a) control, (b) cisplatin treated and (c) colchicine treated. Right panel: (d) control and (e) decay. Each image corresponds to a 1mm by 1mm region. The color bar represents pixel intensity (increasing from left to right) in greyscale OCT images.

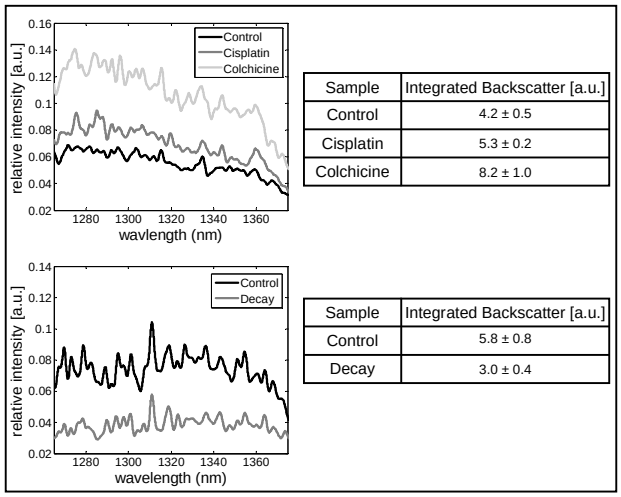

Sample	Integrated Backscatter [a.u.]
Control	4.2 ± 0.5
Cisplatin	5.3 ± 0.2
Colchicine	8.2 ± 1.0

Sample	Integrated Backscatter [a.u.]
Control	5.8 ± 0.8
Decay	3.0 ± 0.4

Fig. 2. Left: Measured relative backscatter power for cisplatin and colchicine treated (top) and decay (bottom) cell samples. Backscatter power normalized to a reference phantom is plotted as a function of wavelength for all cell samples. For each experiment, a corresponding table containing the integrated backscatter values is presented on the right.

Haematoxylin and eosin staining of fixed cells revealed structural differences between the various cell samples. In the control sample, the cells appeared viable, with a large nucleus occupying the majority of the cell volume,

typical of AML cells. The cisplatin treated sample displayed signs of late apoptosis. In over at least 50% of cells we observe either nuclear condensation and/or fragmentation. Some cells also exhibit budding of the membrane, the final stage of apoptotic death. The most striking changes are seen in the colchicine treated cells. Here we observe many cells in mitotic arrest with increased amounts of highly condensed chromatin within the cell. The main feature to be observed in the decay sample is the condensation of the nucleus in many of the cells. It must be noted that H&E staining and light microscopy are limited in their ability to reveal all of the structural changes that may have occurred within these cells as a result of the treatments they underwent, particularly to smaller structures, such as the mitochondria.

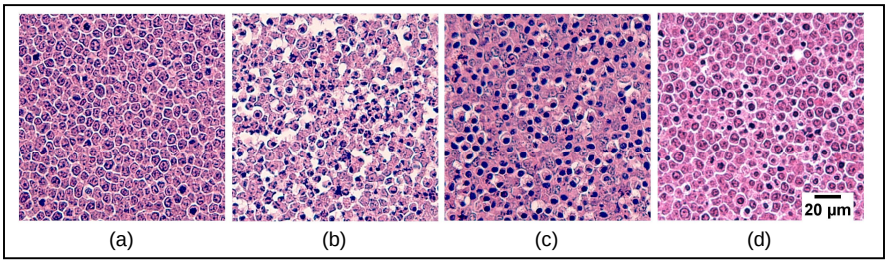

Fig. 3. Haematoxylin and eosin stained sections obtained from (a) untreated (viable) cells, (b) cells treated for 24 hours with cisplatin (apoptotic), (c) cells treated for 24 hours with colchicine (cells in mitotic arrest) and, (d) cells left to decay for 24 hours (oncotic/necrotic). The white spacing in (b) is a retraction artefact typical of apoptotic samples. Average cell/nuclear diameters measured from images in µm were: (a) 8.4 ± 0.8 / 6.6 ± 0.8, (b) 8.5 ± 1.0 / 5.1 ± 2.0 (c) 9.6 ± 1.5 / 4.7 ± 0.8 and (d) 8.9 ± 1.2 / 5.3 ± 1.4.

4. Conclusions

This study demonstrates that it is possible to detect cell death *in vitro* using OCT. Changes in backscatter power spectra and integrated backscatter were linked to structural changes in histology, which from observations were mainly related to the nucleus and overall cell shape. The current results show the potential for differentiating between different modes of cell death using OCT. Further exploration of a relation to changes in smaller cellular structures remains to be made. Correction for light attenuation in cell samples and analysis of OCT signal envelope statistics are in progress. This is the first time, to our knowledge that backscatter spectra and integrated backscatter have been used to detect cell death with OCT *in vitro*. Future work will involve the use of these methods for the characterization of cell death with OCT as well as the further development of these tools for cell death quantification.

5. References

1. F. J. van der Meer, D. J. Faber, M. C. G. Aalders, A. A. Poot, I. Vermes, and T. G. van Leeuwen, "Apoptosis-and necrosis-induced changes in light attenuation measured by optical coherence tomography," Lasers in Medical Science1-9.

2. B. J. Vakoc, R. M. Lanning, J. A. Tyrrell, T. P. Padera, L. A. Bartlett, T. Stylianopoulos, L. L. Munn, G. J. Tearney, D. Fukumura, R. K. Jain, and B. E. Bouma, "Three-dimensional microscopy of the tumor microenvironment in vivo using optical frequency domain imaging," Nat. Med. 15, 1219-1223 (2009).

3. G. J. Czarnota, M. C. Kolios, J. Abraham, M. Portnoy, F. P. Ottensmeyer, J. W. Hunt, and M. D. Sherar, "Ultrasound imaging of apoptosis: high-resolution non-invasive monitoring of programmed cell death in vitro, in situ and in vivo," Br. J. Cancer 81, 520-527 (1999).

4. M. C. Kolios, G. J. Czarnota, M. Lee, J. W. Hunt, and M. D. Sherar, "Ultrasonic spectral parameter characterization of apoptosis," Ultrasound Med. Biol. 28, 589-597 (2002).

5. M. Karbowski and R. J. Youle, "Dynamics of mitochondrial morphology in healthy cells and during apoptosis," Cell Death & Differentiation 10, 870-880 (2003).

6. S. L. Fink and B. T. Cookson, "Apoptosis, pyroptosis, and necrosis: mechanistic description of dead and dying eukaryotic cells," Infect. Immun. 73, 1907 (2005).

7. G. Majno and I. Joris, "Apoptosis, oncosis, and necrosis. An overview of cell death," Am. J. Pathol. 146, 3-15 (1995).

8. D. B. Zamble and S. J. Lippard, "Cisplatin and DNA repair in cancer chemotherapy," Trends Biochem. Sci. 20, 435-439 (1995).

9. G. J. Czarnota, M. C. Kolios, H. Vaziri, S. Benchimol, F. P. Ottensmeyer, M. D. Sherar, and J. W. Hunt, "Ultrasonic biomicroscopy of viable, dead and apoptotic cells," Ultrasound Med. Biol. 23, 961-965 (1997).

10. P. Dustin, *Microtubules* (Springer-Verlag, 1984), 66-76.